Linearized stability analysis of thin-shell wormholes with a cosmological constant

Francisco S N Lobo and Paulo Crawford

Centro de Astronomia e Astrofísica da Universidade de Lisboa, Campo Grande,
Ed C8 1749-016 Lisboa, Portugal

E-mail: flobo@cosmo.fis.fc.ul.pt and crawford@cosmo.fis.fc.ul.pt

Abstract
Spherically symmetric thin-shell wormholes in the presence of a cosmological
constant are constructed applying the cut-and-paste technique implemented
by Visser. Using the Darmois–Israel formalism the surface stresses, which
are concentrated at the wormhole throat, are determined. This construction
allows us to apply a dynamical analysis to the throat, considering linearized
radial perturbations around static solutions. For a large positive cosmological
constant, i.e., for the Schwarzschild–de Sitter solution, the region of stability
is significantly increased, relatively to the null cosmological constant case,
analysed by Poisson and Visser. With a negative cosmological constant, i.e.,
the Schwarzschild–anti de Sitter solution, the region of stability is decreased.
In particular, considering static solutions with a generic cosmological constant,
the weak and dominant energy conditions are violated, while for $a_0 \leqslant 3M$ the
null and strong energy conditions are satisfied. The surface pressure of the
static solution is strictly positive for the Schwarzschild and Schwarzschild–anti
de Sitter spacetimes, but takes negative values, assuming a surface tension
in the Schwarzschild–de Sitter solution, for high values of the cosmological
constant and the wormhole throat radius.

PACS numbers: 04.20.−q, 04.20.Jb, 04.25.−g, 04.90.+e

1. Introduction

Wormhole solutions are necessarily associated with violations of the energy conditions [1],
namely the existence of exotic matter. Being a problematic issue, it is useful to minimize the
usage of exotic matter, although energy condition violations in quantum field theory are well
known [1, 2]. Thus, one may concentrate the exotic matter to a thin shell localized at the
throat, using a simple and elegant class of wormhole solutions implemented by Matt Visser

using the cut-and-paste construction [2–4]. The surface stress-energy tensor components of the exotic matter at the throat are determined, invoking the Darmois–Israel formalism [5, 6].

This construction also permits one to explore a dynamical analysis of the wormhole throat. Poisson and Visser analysed a thin-shell wormhole [7], constructed by pasting together two copies of the Schwarzschild solution at $a > 2M$. Considering a linearized radial perturbation around a static solution, in the spirit of [8, 9], regions of stability were discovered, which lie in a somewhat unexpected patch. This is due to the fact that one does not have a detailed microphysical model for exotic matter, in fact, nothing is known on equations of state of exotic matter. See discussion in Poisson–Visser [7]. Building on this, Eiroa and Romero [10] analysed charged thin-shell wormholes and found that the regions of stability are greatly increased for large values of charge.

The presence of a cosmological constant is also an issue that has been extensively analysed in the literature. For instance, Kim [11] analysed Schwarzschild–de Sitter wormholes, using the cut-and-paste construction. Considering specific equations of state the role of the cosmological constant in the classical and quantum stabilities was studied. This analysis was a natural extension of the Schwarzschild wormhole solution discussed in [4, 12]. Later, Kim and collaborators [13] discussed the $(2 + 1)$-dimensional Schwarzschild–de Sitter wormhole, where once again taking into account specific equations of state, the respective dynamical stability of this type of wormhole was discussed. A comparison with the $(3 + 1)$-dimensional Schwarzschild–de Sitter wormhole and the $(2 + 1)$-dimensional discussed in [14] was established. A partial stability analysis of a $(2 + 1)$-dimensional wormhole solution, in the presence of Λ, was explored by Delgaty and Mann [15], in which the simple case of a constant line energy density was considered.

More recently, prompted by the Randall–Sundrum brane world scenario [16, 17], where our universe is viewed as a domain wall in five-dimensional anti-de Sitter space, Kraus [18] analysed the dynamics of five-dimensional anti-de Sitter domain walls. The motion of the wall was determined using the Darmois–Israel formalism. The possible wall trajectories were described, and the consequences for localized gravity on the wall were examined. Anchordoqui *et al* [19] considered the dynamics of the simple case of one-branes in three-dimensional anti-de Sitter space and generalized the previous analysis for an arbitrary number of dimensions, studying the quantum behaviour within the context of the WKB approximation. Using the standard linearization analysis, Anchordoqui and Olsen [20] studied the classical stability and different behaviours for the expansion of the universe by imposing constraints on the speed of sound, within $(d + 1)$-dimensional anti-de Sitter background spaces. The formation of black holes due to the gravitational collapse of matter trapped on the brane, within the context of the Randall–Sundrum models, was discussed in [21]. Chamblin *et al* conjectured that a non-rotating uncharged black hole on the domain wall is described by a *black cigar* solution in five dimensions. They also considered the five-dimensional Schwarzschild–anti de Sitter solution as another candidate for a black hole formed by the gravitational collapse on a domain wall in anti-de Sitter space. A great deal of attention on the issue of gravity on the brane within the Randall–Sundrum scenario has also been devoted to the cosmological solutions [22–24].

Furthermore, spherically symmetric and static traversable wormholes in the presence of a generic cosmological constant, Λ, were analysed in [25]. A matching of an interior solution to the unique exterior vacuum solution was carried out, and the respective structure and several physical properties and characteristics due to Λ were explored. Specific cases of thin shells at the matching due to the effects of the cosmological constant were studied. In the present paper, we concentrate the exotic matter to the wormhole throat, generalizing the Poisson–Visser analysis for thin-shell wormholes in the presence of a non-vanishing cosmological constant. As in [7, 20] we shall consider linearized radial perturbations around a static wormhole solution,

which is complementary to the analysis discussed by Kim [11]. The advantage of this method lies mainly in the fact that one defines a parametrization of the stability of equilibrium [7, 26], as not to specify an equation of state on the boundary surface. This paper is organized as follows. In section 2 the cut-and-paste construction and the Darmois–Israel formalism are briefly presented, and the surface stresses are deduced. In section 3, a linearized stability analysis is studied in the presence of a generic cosmological constant. Some properties and characteristics of the static solution is also analysed. In section 4 we conclude and in the appendix we briefly consider a linearized stability in $(2 + 1)$-dimensional Schwarzschild–de Sitter thin-shell wormholes.

2. Thin-shell wormholes with a cosmological constant

To generalize the analysis of Poisson–Visser, consider the unique spherically symmetric vacuum solution in the presence of a non-vanishing cosmological constant, i.e.,

$$ds^2 = -\left(1 - \frac{2M}{r} - \frac{\Lambda}{3}r^2\right)dt^2 + \left(1 - \frac{2M}{r} - \frac{\Lambda}{3}r^2\right)^{-1}dr^2 + r^2(d\theta^2 + \sin^2\theta\,d\phi^2). \tag{1}$$

If $\Lambda > 0$, the solution is denoted by the Schwarzschild–de Sitter metric. For $\Lambda < 0$, we have the Schwarzschild–anti de Sitter metric, and of course the specific case of $\Lambda = 0$ is reduced to the Schwarzschild solution. Note that the metric (1) is not asymptotically flat as $r \to \infty$. Rather, it is asymptotically de Sitter, if $\Lambda > 0$, or asymptotically anti-de Sitter, if $\Lambda < 0$. But, considering low values of Λ, the metric is almost flat in the range $M \ll r \ll 1/\sqrt{\Lambda}$. For values below this range, the effects of M dominate, and for values above the range, the effects of Λ dominate, as for large values of the radial coordinate the large-scale structure of the spacetime must be taken into account.

2.1. The Schwarzschild–de Sitter spacetime, $\Lambda > 0$

If $0 < 9\Lambda M^2 < 1$, the factor $f(r) = (1 - 2M/r - \Lambda r^2/3)$ possesses two positive real roots, r_b and r_c, corresponding to the black hole and the cosmological event horizons of the de Sitter spacetime, respectively. Considering the following definitions

$$A = \frac{1}{2M}\sqrt[3]{\frac{3M}{\Lambda}\left(-1 + \sqrt{1 - (9\Lambda M^2)^{-1}}\right)}, \tag{2}$$

$$B = \frac{1}{2M}\sqrt[3]{\frac{3M}{\Lambda}\left(-1 - \sqrt{1 - (9\Lambda M^2)^{-1}}\right)}, \tag{3}$$

we verify that

$$r_b = -M[(A + B) + \sqrt{-3}(A - B)], \tag{4}$$

$$r_c = 2M(A + B), \tag{5}$$

are the black hole and the cosmological event horizons, respectively. Considering $\Lambda M^2 \ll 1$, we have

$$r_b = 2M(1 + 4\Lambda M^2/3), \tag{6}$$

$$r_c = \sqrt{3/\Lambda}(1 - M\sqrt{\Lambda/3}). \tag{7}$$

See [25] for details. If $9\Lambda M^2 = 1$, both horizons coincide at $r_b = r_c = 3M$.

2.2. The Schwarzschild–anti de Sitter spacetime, $\Lambda < 0$

For the Schwarzschild–anti de Sitter metric, with $\Lambda < 0$, the factor $f(r) = (1 - 2M/r + |\Lambda| r^2/3)$ has only one real positive root, r_b, given by

$$r_b = \left(\frac{3M}{|\Lambda|}\right)^{1/3} \left(\sqrt[3]{1 + \sqrt{1 + (9|\Lambda| M^2)^{-1}}} + \sqrt[3]{1 - \sqrt{1 + (9|\Lambda| M^2)^{-1}}}\right), \quad (8)$$

corresponding to a black hole event horizon. For $|\Lambda| M^2 \ll 1$ one obtains

$$r_b = 2M(1 - 4|\Lambda| M^2/3). \tag{9}$$

See [25] for details.

2.3. The Darmois–Israel formalism and the cut-and-paste construction

Given this, we may construct a wormhole solution, using the cut-and-paste technique [2]. Consider two vacuum solutions with Λ and remove from each spacetime the region described by

$$\Omega_{1,2} \equiv \{r_{1,2} \leqslant a | a > r_b\}, \tag{10}$$

where a is a constant and r_b is the black hole event horizon, corresponding to the Schwarzschild–de Sitter and Schwarzschild–anti de Sitter solutions, equations (4) and (8), respectively. The removal of the regions results in two geodesically incomplete manifolds, with boundaries given by the following timelike hypersurfaces

$$\partial\Omega_{1,2} \equiv \{r_{1,2} = a | a > r_b\}. \tag{11}$$

Identifying these two timelike hypersurfaces, $\partial\Omega_1 = \partial\Omega_2$, results in a geodesically complete manifold, with two regions connected by a wormhole and the respective throat situated at $\partial\Omega$. The wormhole connects two regions, asymptotically de Sitter or anti-de Sitter, for $\Lambda > 0$ and $\Lambda < 0$, respectively.

We shall use the Darmois–Israel formalism to determine the surface stresses at the junction boundary [5, 6]. The intrinsic surface stress-energy tensor, S_{ij}, is given by the Lanczos equations [5] in the form $S^i{}_j = -\frac{1}{8\pi}\left(\kappa^i{}_j - \delta^i{}_j \kappa^k{}_k\right)$. For notational convenience, the discontinuity in the second fundamental form or extrinsic curvatures is given by $\kappa_{ij} = K^+_{ij} - K^-_{ij}$. The second fundamental form is defined as

$$K^{\pm}_{ij} = \frac{\partial x^\alpha}{\partial \xi^i} \frac{\partial x^\beta}{\partial \xi^j} \nabla^{\pm}_\alpha n_\beta$$
$$= -n_\gamma \left(\frac{\partial^2 x^\gamma}{\partial \xi^i \partial \xi^j} + \Gamma^{\gamma\pm}_{\alpha\beta} \frac{\partial x^\alpha}{\partial \xi^i} \frac{\partial x^\beta}{\partial \xi^j}\right), \tag{12}$$

where n_γ are the components of the unit normal vector to $\partial\Omega$, and ξ^i represent the intrinsic coordinates in $\partial\Omega$. The superscripts $\pm$ correspond to the exterior and interior spacetimes, respectively. The parametric equation for $\partial\Omega$ is given by $f(x^\mu(\xi^i)) = 0$ and the respective unit 4-normal to $\partial\Omega$ is defined by

$$n_\mu = \pm \left| g^{\alpha\beta} \frac{\partial f}{\partial x^\alpha} \frac{\partial f}{\partial x^\beta} \right|^{-1/2} \frac{\partial f}{\partial x^\mu}, \tag{13}$$

with $n^\mu n_\mu = +1$. The intrinsic metric at $\partial\Omega$ is given by

$$ds^2|_{\partial\Omega} = -d\tau^2 + a^2(\tau)(d\theta^2 + \sin^2\theta \, d\phi^2), \tag{14}$$

where τ is the proper time as measured by a comoving observer on the wormhole throat.

2.4. The surface stresses

Considerable simplifications occur due to spherical symmetry, namely

$$\kappa^i{}_j = \mathrm{diag}\left(\kappa^\tau{}_\tau, \kappa^\theta{}_\theta, \kappa^\theta{}_\theta\right).$$

Thus, the surface stress-energy tensor may be written in terms of the surface energy density, σ, and the surface pressure, p, as

$$S^i{}_j = \mathrm{diag}(-\sigma, p, p),$$

which taking into account the Lanczos equations, reduce to

$$\sigma = -\frac{1}{4\pi}\kappa^\theta{}_\theta, \tag{15}$$

$$p = \frac{1}{8\pi}\left(\kappa^\tau{}_\tau + \kappa^\theta{}_\theta\right). \tag{16}$$

This simplifies the determination of the surface stress-energy tensor to that of the calculation of the non-trivial components of the extrinsic curvature.

The imposition of spherical symmetry is sufficient to conclude that there is no gravitational radiation, independently of the behaviour of the wormhole throat. The position of the throat is given by $x^\mu(\tau, \theta, \phi) = (t(\tau), a(\tau), \theta, \phi)$, and the respective 4-velocity is

$$U^\mu = \left(\frac{\sqrt{1 - 2M/a - \Lambda a^2/3 + \dot{a}^2}}{1 - 2M/a - \Lambda a^2/3}, \dot{a}, 0, 0\right), \tag{17}$$

where the overdot denotes a derivative with respect to τ.

The unit normal to the throat may be determined by equation (13) or by the contractions, $U^\mu n_\mu = 0$ and $n^\mu n_\mu = +1$, and is given by

$$n^\mu = \left(\frac{\dot{a}}{1 - 2M/a - \Lambda a^2/3}, \sqrt{1 - 2M/a - \Lambda a^2/3 + \dot{a}^2}, 0, 0\right). \tag{18}$$

Using equations (1), (12) and (18), the non-trivial components of the extrinsic curvature are given by

$$K^{\theta\pm}{}_\theta = \pm\frac{1}{a}\sqrt{1 - 2M/a - \Lambda a^2/3 + \dot{a}^2}, \tag{19}$$

$$K^{\tau\pm}{}_\tau = \pm\frac{M/a^2 - \Lambda a/3 + \ddot{a}}{\sqrt{1 - 2M/a - \Lambda a^2/3 + \dot{a}^2}}. \tag{20}$$

Thus, the Einstein field equations, equations (15), (16), with equations (19), (20), then provide us with the following surface stresses

$$\sigma = -\frac{1}{2\pi a}\sqrt{1 - 2M/a - \Lambda a^2/3 + \dot{a}^2}, \tag{21}$$

$$p = \frac{1}{4\pi a}\frac{1 - M/a - 2\Lambda a^2/3 + \dot{a}^2 + a\ddot{a}}{\sqrt{1 - 2M/a - \Lambda a^2/3 + \dot{a}^2}}. \tag{22}$$

We also verify that the above equations imply the conservation of the surface stress-energy tensor

$$\dot{\sigma} = -2\left(\sigma + p\right)\frac{\dot{a}}{a}, \tag{23}$$

or

$$\frac{\mathrm{d}(\sigma A)}{\mathrm{d}\tau} + p \frac{\mathrm{d}A}{\mathrm{d}\tau} = 0, \tag{24}$$

where $A = 4\pi a^2$ is the area of the wormhole throat. The first term represents the variation of the internal energy of the throat, and the second term is the work done by the throat's internal forces.

3. Linearized stability analysis

Equation (21) may be recast into the following dynamical form:

$$\dot{a}^2 - \frac{2M}{a} - \frac{\Lambda}{3}a^2 - (2\pi\sigma a)^2 = -1, \tag{25}$$

which determines the motion of the wormhole throat. Considering an equation of state of the form, $p = p(\sigma)$, the energy conservation, equation (23), can be integrated to yield

$$\ln(a) = -\frac{1}{2} \int \frac{\mathrm{d}\sigma}{\sigma + p(\sigma)}. \tag{26}$$

This result, formally inverted to provide $\sigma = \sigma(a)$, can be finally substituted into equation (25). Equation (25) can also be written as $\dot{a}^2 = -V(a)$, with the potential defined as

$$V(a) = 1 - \frac{2M}{a} - \frac{\Lambda}{3}a^2 - (2\pi\sigma a)^2. \tag{27}$$

3.1. Static solution

One may explore specific equations of state, but following the Poisson–Visser reasoning [7], we shall consider a linear perturbation around a static solution with radius a_0. The respective values of the surface energy density and the surface pressure, at a_0, are given by

$$\sigma_0 = -\frac{1}{2\pi a_0}\sqrt{1 - 2M/a_0 - \Lambda a_0^2/3}, \tag{28}$$

$$p_0 = \frac{1}{4\pi a_0}\frac{1 - M/a_0 - 2\Lambda a_0^2/3}{\sqrt{1 - 2M/a_0 - \Lambda a_0^2/3}}. \tag{29}$$

One verifies that the surface energy density is always negative, implying the violation of the weak and dominant energy conditions.

The null energy condition is satisfied if $\sigma_0 + p_0 \geqslant 0$. Taking into account the following relationship

$$\sigma_0 + p_0 = -\frac{1}{4\pi a_0}\frac{1 - 3M/a_0}{\sqrt{1 - 2M/a_0 - \Lambda a_0^2/3}}, \tag{30}$$

the null energy condition is satisfied for $a_0 \leqslant 3M$, considering a generic cosmological constant.

The strong energy condition is satisfied if $\sigma_0 + p_0 \geqslant 0$ and $\sigma_0 + 2p_0 \geqslant 0$, and by continuity implies the null energy condition. Consider

$$\sigma_0 + 2p_0 = \frac{1}{2\pi a_0}\frac{M/a_0 - \Lambda a_0^2/3}{\sqrt{1 - 2M/a_0 - \Lambda a_0^2/3}}. \tag{31}$$

For the Schwarzschild and the Schwarzschild–anti de Sitter spacetimes, $\Lambda \leqslant 0$ and $M > 0$, the condition $\sigma_0 + 2p_0 > 0$ is verified. The Schwarzschild–de Sitter solution, $\Lambda > 0$, requires
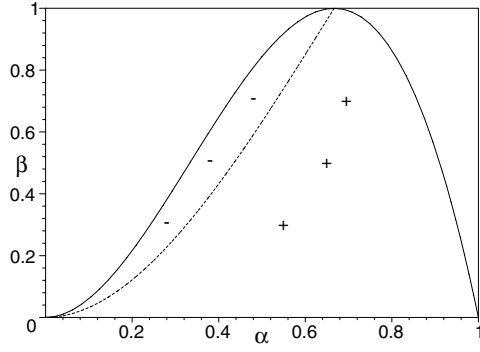
Figure 1. We have defined $\alpha = 2M/a_0$ and $\beta = 9\Lambda M^2$. Only the region below the solid line is considered. The dashed line depicts a null surface pressure. To the right of the dashed curve we have a surface pressure, and to the left a surface tension. See text for details.

a further analysis. Exercising simple algebraic gymnastics, we verify that the imposition of $a_0 \leqslant 3M$, so that the null energy condition is satisfied, and taking into account $9\Lambda M^2 < 1$, implies $M/a_0 > \Lambda a_0^2/3$, so that $\sigma_0 + 2p_0 > 0$. We conclude that the null and strong energy conditions are satisfied for $a_0 \leqslant 3M$ for a generic Λ. In particular, for $M = 0$ and $\Lambda = 0$, the above analysis is reduced to the Minkowski surgery discussed in [2], in which all the pointwise and averaged energy conditions are violated for a convex section of the wormhole throat. For $M = 0$ and $\Lambda \neq 0$, the de Sitter and the anti-de Sitter solutions, considering equations (28) and (30) all the energy conditions are also violated.

An analysis of the sign of p_0, equation (29), is also in order. For the Schwarzschild and the Schwarzschild–anti de Sitter solutions, $\Lambda \leqslant 0$, p_0 is positive, implying a surface pressure. But, for the Schwarzschild–de Sitter spacetime p_0 may have a negative value, assuming the character of a surface tension. The sign of p_0 is analysed in figure 1, where we plot $9\Lambda M^2 \times 2M/a_0$. For large values of the cosmological constant, or for large M, and for large values of a_0, one verifies that a surface tension is needed to support the structure. This is somehow to be expected because for high values of Λ the large-scale curvature of the solution has to be taken into account. Therefore, one needs a tension to hold the wormhole from expanding. For low values of Λ and for small a_0, p_0 is a surface pressure, preventing the wormhole from collapsing. The qualitative behaviour of p_0 is similar to the surface pressure/tension for the thin shells considered in [25].

The behaviour of the sign becomes transparent in the following algebraic analysis. Consider the factors given by $f(a_0) = \left(1 - 2M/a_0 - \Lambda a_0^2/3\right)$ and $h(a_0) = \left(1 - M/a_0 - 2\Lambda a_0^2/3\right)$. Define $\alpha = 2M/a_0$ and $\beta = 9\Lambda M^2$, so that $\beta = 27\alpha^2(1-\alpha)/4$ is considered for $f(a_0) = 0$, which is depicted as a solid line in figure 1. p_0 will be null if $h(a_0) = 0$, i.e., for $9\Lambda M^2 = 27\alpha^2(1-\alpha/2)/8$, depicted as a dashed line in figure 1. A surface pressure is present, $p_0 > 0$, if $h(a_0) > 0$, which is shown to the right of the dashed curve in figure 1. A surface tension, $p_0 < 0$, is shown to the left of the dashed line.

3.2. Linearization analysis

Linearizing around the stable solution at $a = a_0$, we consider a Taylor expansion of $V(a)$ around a_0 to second order, which provides

$$V(a) = V(a_0) + V'(a_0)(a - a_0) + \tfrac{1}{2}V''(a_0)(a - a_0)^2 + O[(a - a_0)^3], \quad (32)$$

where the prime denotes a derivative with respect to a, $\mathrm{d}/\mathrm{d}a$.

To determine the first and second derivatives of the potential equation (27), $V'(a)$ and $V''(a)$, respectively, it is useful to rewrite the conservation of the surface stress-energy tensor, equation (23), as $\sigma' a = -2(\sigma + p)$, taking into account $\sigma' = \dot{\sigma}/\dot{a}$. Defining the parameter $\eta(\sigma) = \mathrm{d}p/\mathrm{d}\sigma = p'/\sigma'$, we have $\sigma' + 2p' = \sigma'(1 + 2\eta)$. The physical interpretation of η is discussed in [7], and $\sqrt{\eta}$ is normally interpreted as the speed of sound. With these results, $V'(a)$ and $V''(a)$ are, respectively, given by

$$V'(a) = \frac{2M}{a^2} - \frac{2\Lambda}{3}a + 8\pi^2 \sigma a(\sigma + 2p), \tag{33}$$

$$V''(a) = -\frac{4M}{a^3} - \frac{2\Lambda}{3} - 8\pi^2[(\sigma + 2p)^2 + 2\sigma(\sigma + p)(1 + 2\eta)]. \tag{34}$$

Evaluated at the static solution, at $a = a_0$, using equations (28), (29) and taking into account equations (30) and (31), we readily find $V(a_0) = 0$ and $V'(a_0) = 0$, with $V''(a_0)$ given by

$$V''(a_0) = -\frac{2}{a_0^2}\left[\frac{2M}{a_0} + \frac{\Lambda}{3}a_0^2 + \frac{\left(M/a_0 - \Lambda a_0^2/3\right)^2}{1 - 2M/a_0 - \Lambda a_0^2/3} + (1 + 2\eta_0)\left(1 - \frac{3M}{a_0}\right)\right], \tag{35}$$

where $\eta_0 = \eta(\sigma_0)$.

The potential $V(a)$, equation (32), is reduced to

$$V(a) = \tfrac{1}{2}V''(a_0)(a - a_0)^2 + O[(a - a_0)^3], \tag{36}$$

so that the equation of motion for the wormhole throat presents the following form

$$\dot{a}^2 = -\tfrac{1}{2}V''(a_0)(a - a_0)^2 + O[(a - a_0)^3], \tag{37}$$

to the order of approximation considered. If $V''(a_0) < 0$ is verified, then the potential $V(a_0)$ has a local maximum at a_0, where a small perturbation in the wormhole throat's radius will provoke an irreversible contraction or expansion of the throat. Thus, the solution is stable if and only if $V(a_0)$ has a local minimum at a_0 and $V''(a_0) > 0$, i.e.,

$$\frac{2M}{a_0} + \frac{\Lambda}{3}a_0^2 + \frac{\left(M/a_0 - \Lambda a_0^2/3\right)^2}{1 - 2M/a_0 - \Lambda a_0^2/3} + (1 + 2\eta_0)\left(1 - \frac{3M}{a_0}\right) < 0, \tag{38}$$

or

$$\eta_0\left(1 - \frac{3M}{a_0}\right) < -\frac{1 - 3M/a_0 + 3M^2/a_0^2 - \Lambda M a_0}{2\left(1 - 2M/a_0 - \Lambda a_0^2/3\right)}. \tag{39}$$

We need to analyse equation (39) for several cases. Firstly, for the Schwarzschild–de Sitter solution, $\Lambda > 0$, we are only interested in the range $r_b < a_0 < r_c$, with r_b and r_c given by equations (4) and (5), respectively. The factor $g(a_0) = \left(1 - 3M/a_0 + 3M^2/a_0^2 - \Lambda M a_0\right)$ has only one positive root, a_r, so that $g(a_0) > 0$ for $a_0 < a_r$, and $g(a_0) < 0$ for $a_0 > a_r$. It is a simple matter to prove that $a_r > r_c$, i.e., the value for which the factor $g(a_0)$ becomes negative is greater than the cosmological horizon, r_c. In particular, if $\Lambda M^2 \ll 1$, we verify that $a_r \gg r_c$. For transparency, consider the following algebraic analysis, analogous to the one preceding figure 1. Consider the factor $f(a_0) = \left(1 - 2M/a_0 - \Lambda a_0^2/3\right)$. Define $\alpha = 2M/a_0$ and $\beta = 9\Lambda M^2$, so that $\beta = 27\alpha^2(1 - \alpha)/4$ is considered for $f(a_0) = 0$, depicted as a solid line in figure 2. $g(a_0) = 0$ or $9\Lambda M^2 = 2\alpha(1 - 3\alpha/2 + 3\alpha^2/4)/9$ is shown as a dashed line in figure 2. The region of values for which $g(a_0) > 0$ is depicted below the dashed line, which covers the entire area of interest. Thus, the left-hand side of equation (39) in the range of interest, $r_b < a_0 < r_c$, is strictly negative.

Secondly, for the Schwarzschild–anti de Sitter spacetime, $\Lambda < 0$, we verify that the factor $h(a_0) = \left(1 - 3M/a_0 + 3M^2/a_0^2 + |\Lambda|M a_0\right)$ is always positive.
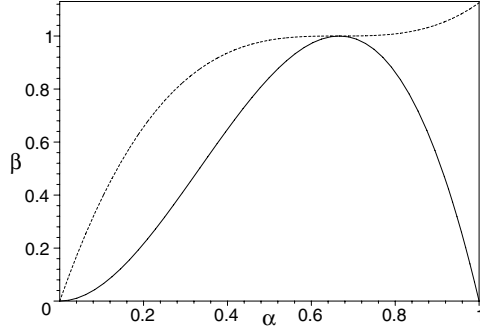
Figure 2. We have defined $\alpha = 2M/a_0$ and $\beta = 9\Lambda M^2$. Only the region below the solid line is considered. The region of values for which $g(a_0) > 0$ is depicted below the dashed line. See text for details.

Thirdly, if $M = 0$ and $\Lambda \neq 0$, the solution reduces to the de Sitter spacetime, if $\Lambda > 0$, and to the anti-de Sitter, if $\Lambda < 0$, we verify that the right-hand side of equation (39) is always negative. If $\Lambda = 0$ and $M \neq 0$, the analysis is reduced to the Schwarzschild solution, considered by Poisson and Visser [7].

Therefore, for all the cases considered above, the right-hand side of equation (39) is always negative, while the left-hand side changes sign at $a_0 = 3M$. Thus, one deduces that the stability regions are dictated by the following inequalities

$$\eta_0 < -\frac{1 - 3M/a_0 + 3M^2/a_0^2 - \Lambda M a_0}{2\left(1 - 2M/a_0 - \Lambda a_0^2/3\right)\left(1 - 3M/a_0\right)}, \qquad a_0 > 3M, \qquad (40)$$

$$\eta_0 > -\frac{1 - 3M/a_0 + 3M^2/a_0^2 - \Lambda M a_0}{2\left(1 - 2M/a_0 - \Lambda a_0^2/3\right)\left(1 - 3M/a_0\right)}, \qquad a_0 < 3M. \qquad (41)$$

One may analyse several cases.

*3.2.1. De Sitter spacetime.* For the de Sitter spacetime, with $M = 0$ and $\Lambda > 0$, equation (39) reduces to

$$\eta_0 < -\frac{1}{2\left(1 - \Lambda a_0^2/3\right)}, \qquad \text{for} \quad 0 < a_0 < \sqrt{3/\Lambda}. \qquad (42)$$

The stability region is depicted in the left-hand plot of figure 3.

*3.2.2. Anti-de Sitter spacetime.* For the anti-de Sitter spacetime, with $M = 0$ and $\Lambda < 0$, equation (39) gives

$$\eta_0 < -\frac{1}{2\left(1 + |\Lambda| a_0^2/3\right)}, \qquad \text{for} \quad a_0 > 0, \qquad (43)$$

and the respective stability region is depicted in the right-hand plot of figure 3. As mentioned in the introduction, a negative cosmological constant plays an important role in the Randall–Sundrum models [16, 17]. Anchordoqui and Olsen [20] considered the dynamics of a d-dimensional brane world sweeping through the $(d + 1)$-dimensional bulk, by imposing constraints on the brane world cosmologies and considering that $V''(a_0) < 0$, so that $V(a_0)$ is a local maximum at a_0. In particular, they analysed different behaviours for the expansion
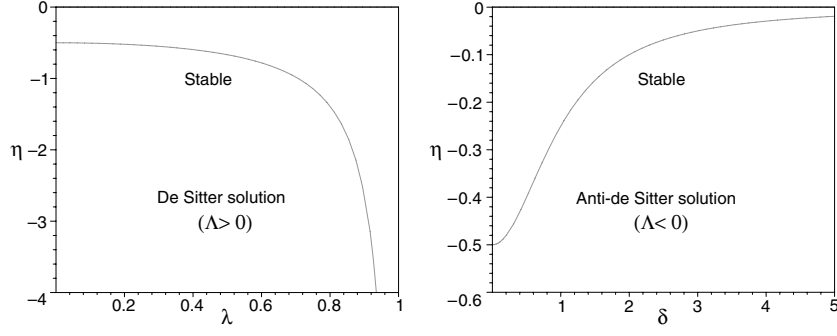
Figure 3. We have defined $\lambda = a_0/(3/\Lambda)^{1/2}$ and $\delta = a_0/(3/|\Lambda|)^{1/2}$, respectively. The regions of stability are depicted in the graphs, below the curves for the de-Sitter and the anti-de Sitter solutions, respectively.
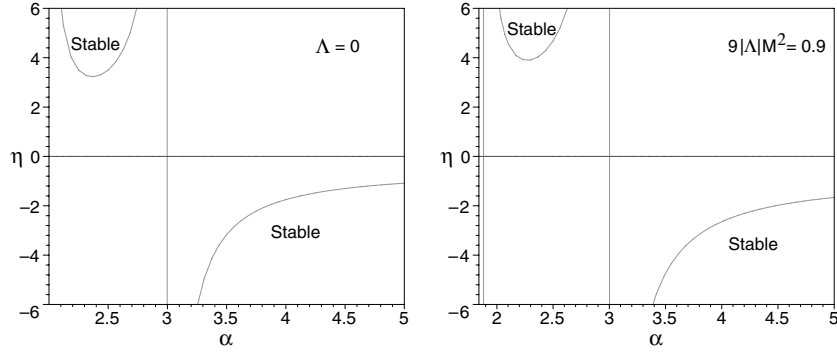
Figure 4. We have defined $\alpha = a_0/2M$. The regions of stability are depicted for the Schwarzschild and the Schwarzschild–anti de Sitter solutions, respectively. Imposing the value $9|\Lambda|M^2 = 0.9$ in the Schwarzschild–anti de Sitter case, we verify that the stability regions decrease relatively to the Schwarzschild solution.

of the universe by imposing constraints on the speed of sound. But, in the presence of exotic matter one cannot naively interpret η_0 as the speed of sound on the wormhole throat. Therefore the plots that we have considered generally extend beyond $0 < \eta_0 \leqslant 1$. Equation (43) may be readily obtained from the Anchordoqui–Olsen linearized stability analysis by setting $d = 3$ and considering that $V(a_0)$ is a local minimum so that $V''(a_0) > 0$.

3.2.3. Schwarzschild spacetime. This is the particular case of the Poisson–Visser analysis [7], with $\Lambda = 0$, which reduces to

$$\eta_0 < -\frac{1 - 3M/a_0 + 3M^2/a_0^2}{2(1 - 2M/a)(1 - 3M/a_0)}, \qquad a_0 > 3M, \tag{44}$$

$$\eta_0 > -\frac{1 - 3M/a_0 + 3M^2/a_0^2}{2(1 - 2M/a)(1 - 3M/a_0)}, \qquad a_0 < 3M. \tag{45}$$

The stability regions are shown in the left-hand plot of figure 4.
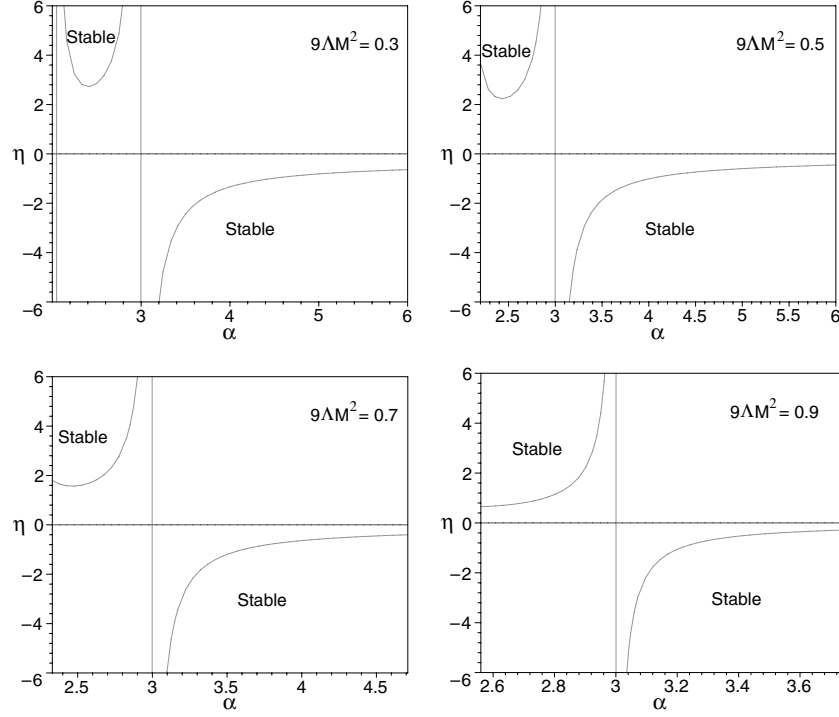
Figure 5. We have defined $\alpha = a_0/2M$. The regions of stability for the Schwarzschild–de Sitter solution, imposing $9\Lambda M^2 = 0.3$, $9\Lambda M^2 = 0.5$, $9\Lambda M^2 = 0.7$ and $9\Lambda M^2 = 0.9$, respectively. The regions of stability are significantly increased, relatively to the $\Lambda = 0$ case, for increasing values of $9\Lambda M^2$.

3.2.4. Schwarzschild–anti de Sitter spacetime. For the Schwarzschild–anti de Sitter spacetime, with $\Lambda < 0$, we have

$$\eta_0 < -\frac{1 - 3M/a_0 + 3M^2\big/a_0^2 + |\Lambda|Ma_0}{2\big(1 - 2M/a_0 + |\Lambda|a_0^2\big/3\big)(1 - 3M/a_0)}, \qquad a_0 > 3M, \qquad (46)$$

$$\eta_0 > -\frac{1 - 3M/a_0 + 3M^2\big/a_0^2 + |\Lambda|Ma_0}{2\big(1 - 2M/a_0 + |\Lambda|a_0^2\big/3\big)(1 - 3M/a_0)}, \qquad a_0 < 3M. \qquad (47)$$

The regions of stability are depicted in the right-hand plot of figure 4, considering the value $9|\Lambda|M^2 = 0.9$. In this case, the black hole event horizon is given by $r_b \simeq 1.8M$. We verify that the regions of stability decrease, relatively to the Schwarzschild case.

Various aspects of the five-dimensional Schwarzschild–anti de Sitter solution were treated in [18, 21]. Kraus considered [18] the dynamics of anti-de Sitter domain wall with a static bulk, by deducing equations of motion of the wall applying the Darmois–Israel formalism. Observers on the wall interpret the motion of the wall through the static background as a cosmological expansion or contraction. One may generalize the $(d + 1)$-dimensional anti-de Sitter Anchordoqui–Olsen linearized stability analysis [20] to the $(d + 1)$-dimensional Schwarzschild–anti de Sitter solution, and obtain equations (46), (47) by setting $d = 3$.

3.2.5. Schwarzschild–de Sitter spacetime. For the Schwarzschild–de Sitter spacetime, with $\Lambda > 0$, we have

$$\eta_0 < -\frac{1 - 3M/a_0 + 3M^2/a_0^2 - \Lambda M a_0}{2(1 - 2M/a_0 - \Lambda a_0^2/3)(1 - 3M/a_0)}, \qquad a_0 > 3M, \tag{48}$$

$$\eta_0 > -\frac{1 - 3M/a_0 + 3M^2/a_0^2 - \Lambda M a_0}{2(1 - 2M/a_0 - \Lambda a_0^2/3)(1 - 3M/a_0)}, \qquad a_0 < 3M. \tag{49}$$

The regions of stability are depicted in figure 5 for increasing values of $9\Lambda M^2$. In particular, for $9\Lambda M^2 = 0.7$ the black hole and cosmological horizons are given by $r_b \simeq 2.33M$ and $r_c = 4.71M$, respectively. Thus, only the interval $2.33 < a_0/M < 4.71$ is taken into account, as shown in the range of the respective plot. Analogously, for $9\Lambda M^2 = 0.9$, we find $r_b \simeq 2.56M$ and $r_c = 3.73M$. Therefore only the range within the interval $2.56 < a_0/M < 3.73$ corresponds to the stability regions, also shown in the respective plots.

We verify that for large values of Λ, or large M, the regions of stability are significantly increased, relatively to the $\Lambda = 0$ case.

4. Conclusion

The traditional manner of solving the Einstein field equation consists in considering a plausible stress-energy tensor and finding the respective geometrical structure. Specifically, physically plausible equations of state are derived for the respective pressures as a function of the energy density, and using the Einstein field equation, the respective metric is determined. In considering wormhole solutions, the Einstein field equation is run in the reverse direction by imposing an exotic metric, $g_{\mu\nu}$, and eventually the matter source for the respective geometry is found. In this manner, solutions involving the violation of the energy conditions have been found. However, up to date a detailed microphysical model describing the physics of exotic matter does not exist, i.e., nothing is known on equations of state of exotic matter. Under normal circumstances the parameter $\sqrt{\eta_0}$ is interpreted as the speed of sound, but in the presence of exotic matter this cannot naively be done so. Consequently, one cannot *a priori* impose $0 < \eta_0 \leqslant 1$, as there are several known examples of exotic $\eta_0 < 0$ behaviour, namely the Casimir effect and the false vacuum. See [7] for a detailed analysis. Therefore, the conditions $\eta_0 > 1$ and $\eta_0 < 0$ cannot be ruled out, until a detailed microphysical model of exotic matter is devised.

However, we have found that for large positive values of Λ, i.e., the Schwarzschild–de Sitter solution, the regions of stability significantly increase relatively to the case analysed by Poisson and Visser, imposing less severe restrictions on η_0. For negative values of Λ, i.e., the Schwarzschild–anti de Sitter, the regions of stability decrease.

Appendix. Linearized stability in (2 + 1)-dimensional Schwarzschild–de Sitter thin-shell wormholes

It is interesting to analyse the (2 + 1)-dimensional Schwarzschild–de Sitter solution [13]. The metric is given by

$$ds^2 = -\frac{(1 - 4M - \Lambda r^2)}{1 - 4M} dt^2 + \frac{dr^2}{1 - 4M - \Lambda r^2} + r^2 d\phi^2. \tag{A.1}$$

For $1 - 4M \geqslant 0$, an event horizon appears at $r_b = \sqrt{(1 - 4M)/\Lambda}$. We shall only consider the static spacetime, with $r < r_b$.

If $\Lambda = 0$, equation (A.1) is reduced to the $(2 + 1)$-dimensional Schwarzschild metric,

$$ds^2 = -dt^2 + \frac{dr^2}{1 - 4M} + r^2\, d\phi^2. \tag{A.2}$$

The properties and characteristics of the metric (A.2) are discussed in [13, 14].

Considering $M = 0$, equation (A.1) reduces to the $(2 + 1)$-dimensional de Sitter metric, given by

$$ds^2 = -(1 - \Lambda r^2)\, dt^2 + \frac{dr^2}{1 - \Lambda r^2} + r^2\, d\phi^2. \tag{A.3}$$

Considering the cut-and-paste construction described in section 2.3, the Lanczos equations in $(2 + 1)$ dimensions reduce to

$$\sigma = -\frac{1}{8\pi} \kappa^{\theta}{}_{\theta}, \tag{A.4}$$

$$p = +\frac{1}{8\pi} \kappa^{\tau}{}_{\tau}. \tag{A.5}$$

The extrinsic curvatures are given by

$$K^{\theta\,\pm}_{\;\;\theta} = \pm\frac{1}{a}\sqrt{1 - 4M - \Lambda a^2 + \dot{a}^2}, \tag{A.6}$$

$$K^{\tau\,\pm}_{\;\;\tau} = \pm\frac{-\Lambda a + \ddot{a}}{\sqrt{1 - 4M - \Lambda a^2 + \dot{a}^2}}, \tag{A.7}$$

and equations (A.4), (A.5) take the following form

$$\sigma = -\frac{1}{4\pi a}\sqrt{1 - 4M - \Lambda a^2 + \dot{a}^2}, \tag{A.8}$$

$$p = -\frac{1}{4\pi a}\frac{\Lambda a^2 - a\ddot{a}}{\sqrt{1 - 4M - \Lambda a^2 + \dot{a}^2}}. \tag{A.9}$$

The conservation of the line stress-energy tensor implies

$$\dot{\sigma} = -(\sigma + p)\frac{\dot{a}}{a} \tag{A.10}$$

or

$$\frac{d(\sigma l)}{d\tau} + p\frac{dl}{d\tau} = 0, \tag{A.11}$$

where $l = 2\pi a$ is the circumference of the stress-energy ring .

The equation of motion of the wormhole throat, deduced from equation (A.8), takes the following form

$$\dot{a}^2 - 4M - \Lambda a^2 - (4\pi a\sigma)^2 = -1, \tag{A.12}$$

or by $\dot{a}^2 = -V(a)$, with the potential defined as

$$V(a) = 1 - 4M - \Lambda a^2 - (4\pi a\sigma)^2. \tag{A.13}$$

Linearizing around the stable solution at $a = a_0$, consider the Taylor expansion of $V(a)$ around a_0 to second order in section 3.2. The static line energy density and line pressure

are given by

$$\sigma_0 = -\frac{1}{4\pi a_0}\sqrt{1 - 4M - \Lambda a_0^2}, \tag{A.14}$$

$$p_0 = -\frac{1}{4\pi a_0}\frac{\Lambda a_0^2}{\sqrt{1 - 4M - \Lambda a_0^2}}. \tag{A.15}$$

Considering equation (32), the first and second derivatives of $V(a)$, are

$$V'(a) = -2\Lambda a + 32\pi^2 a\sigma p, \tag{A.16}$$

$$V''(a) = -2\Lambda - 32\pi^2[p^2 + \sigma(\sigma + p)\eta], \tag{A.17}$$

taking into account the definition $\eta(\sigma) = p'/\sigma'$ and rewriting the conservation of the line stress-energy tensor, equation (A.10), as $\sigma'a = -(\sigma + p)$, with $\sigma' = \dot{\sigma}/\dot{a}$.

Evaluated at the static solution, at $a = a_0$, we readily find $V(a_0) = 0$ and $V'(a_0) = 0$, with $V''(a_0)$ given by

$$V''(a_0) = -\frac{2}{a_0^2}(1 - 4M)\left(\frac{\Lambda a_0^2}{1 - 4M - \Lambda a_0^2} + \eta_0\right). \tag{A.18}$$

The solution is stable if and only if $V''(a_0) > 0$, or

$$\eta_0 < -\frac{\Lambda a_0^2}{1 - 4M - \Lambda a_0^2}. \tag{A.19}$$

References

[1] Morris M S and Thorne K S 1988 *Am. J. Phys.* **56** 395
[2] Visser M 1995 *Lorentzian Wormholes: From Einstein to Hawking* (New York: AIP)
[3] Visser M 1989 *Phys. Rev.* D **39** 3182
[4] Visser M 1989 *Nucl. Phys.* B **328** 203
[5] Israel W 1966 *Nuovo Cimento* B **44** 1
[6] Papapetrou A and Hamoui A 1968 *Ann. Inst. Henri Poincaré* **9** 179
[7] Poisson E and Visser M 1995 *Phys. Rev.* D **52** 7318 (*Preprint* gr-qc/9506083)
[8] Brady P R, Louko J and Poisson E 1991 *Phys. Rev.* D **44** 1891
[9] Balbinot R and Poisson E 1990 *Phys. Rev.* D **41** 395
[10] Eiroa E F and Romero G E 2003 Linearized stability of charged thin-shell wormholes *Preprint* gr-qc/0303093
[11] Kim S W 1992 *Phys. Lett.* B **166** 13
[12] Visser M 1990 *Phys. Lett.* B **242** 24
[13] Kim S W, Lee H, Kim S K and Yang J 1993 *Phys. Lett.* A **183** 359
[14] Perry G P and Mann R B 1992 *Gen. Rel. Grav.* **24** 305
[15] Delgaty M S R and Mann R B 1995 *Int. J. Mod. Phys.* D **4** 231 (*Preprint* gr-qc/9404046)
[16] Randall L and Sundrum R 1999 *Phys. Rev. Lett.* **83** 3370 (*Preprint* hep-ph/9905221)
[17] Randall L and Sundrum R 1999 *Phys. Rev. Lett.* **83** 4690 (*Preprint* hep-ph/9906064)
[18] Kraus P 1999 *J. High Energy Phys.* JHEP12(1999)011 (*Preprint* hep-th/9910149)
[19] Anchordoqui L, Nuñez C and Olsen K 2000 *J. High Energy Phys.* JHEP10(2000)050 (*Preprint* hep-th/0007064)
[20] Anchordoqui L and Olsen K 2001 *Mod. Phys. Lett.* A **18** 1157 (*Preprint* hep-th/0008102)
[21] Chamblin A, Hawking S W and Reall H S 2000 *Phys. Rev.* D **61** 065007 (*Preprint* hep-th/9909205)
[22] Garriga J and Sasaki M 2000 *Phys. Rev.* D **62** 043523 (*preprint* hep-th/9912118)
[23] Kaloper N 1999 *Phys. Rev.* D **60** 123506 (*preprint* hep-th/9905210)
[24] Binétruy P, Deffayet C, Ellwanger U and Langlois D 2000 *Phys. Lett.* B **477** 285 (*preprint* hep-th/9910219)
[25] Lemos J P S, Lobo F S N and de Oliveira S Q 2003 Morris-Thorne wormholes with a cosmological constant   **See endnote 1**
     Preprint gr-qc/0302049 (*Phys. Rev.* D at press)
[26] Ishak M and Lake K 2002 *Phys. Rev.* D **65** 044011 (*Preprint* gr-qc/0108058)

Endnotes

(1) Author: Please update reference [25].